Supporting Information

Super-zincophilic Electrolyte Additive Enables Long-life Zn Anode under High Current Density and Areal Capacity

Yaheng Geng,[a] Licheng Miao,[b] Zichao Yan,*[a] Wenli Xin,[a] Lei Zhang,[a] Huiling Peng,[a] Junwei Li,[a] Zhiqiang Zhu*[a]

[a] State Key Laboratory of Chemo/Biosensing and Chemometrics, College of Chemistry and Chemical Engineering, Hunan University, Changsha 410082, China

[b] Key Laboratory of Optoelectronic Devices and Systems of Ministry of Education and Guangdong Province, College of Physics and Optoelectronic Engineering, Shenzhen University, Shenzhen 518060, China

*Corresponding authors.

E-mail addresses: zcyan@hnu.edu.cn (Zichao Yan); zqzhu@hnu.edu.cn (Zhiqiang Zhu)

1. Experimental and Computational section

1.1 Materials

Zinc sulphate (ZnSO$_4$, 99%) and di-2-picolylamine (DPA, 97%) were purchased from Shanghai Macklin Biochemcal Co., Ltd. All electrolytes were prepared by molarity, and the electrolytes with different concentrated DPA is defined as x μL mL^{-1}, representing that x μL DPA was added to each milliliter of 2M ZnSO$_4$ aqueous solution. The water is purified by the Laboratory water purification system (Eco-S15Q, Hitech Instruments Co., Ltd). The polyaniline (PANI) cathode was prepared through a previously reported method.[1] Typically, 1.85 mL of aniline (≥95%, Macklin Biochemcal Co., Ltd.) monomer was added into 100 mL of HCl solution (1 M) under string, and then commercial carbon felts were dipped into the solution (0 °C in an ice bath). After string for 1 h, 30 mL of HCl (1 M) containing 1.14 g of ammonium persulfate (98.5%, Macklin Biochemcal Co., Ltd.) was added into above solution under ice bath. After reaction continued for 1 h, the target materials were obtained by washing the carbon felts with pure water, and then drying at 80 °C.

1.2 Materials characterizations

IR spectra were recorded on SHIMADZU IR Spirit-T and reported in unit of cm^{-1}. Raman spectra were recorded using a Raman microscope (Renishaw plc (invia-reflex)) with a 532 nm diode laser. The photoluminesence spectra of various electrolytes (aqueous solution) were recorded on a Thermo Scientific Lumina. A Nikon (Ti-E+A1 SI) confocal laser scanning microscope with the excited light of 405 nm was used to record the fluorescence signal on the zinc anode after cycling in the ZSO and ZSPA electrolyte. Scanning electron microscopy (SEM) images were obtained using Oxford Ultim-Max 40. The morphology of the Zn electrodes was characterized by a 3D Laser Confocal Scanning Microscope (LCSM, Leica TCS SP8 SR). X-ray diffraction (XRD) patterns were recorded by PANalytical Empyren X-ray diffractometer with Cu K$_\alpha$ radiation (45kV and 40mA). Real-time observations of Zn deposition on Zn foil were performed by optical microscope (Fenghuang PH50-1B43L-A/PL).

1.3 Electrochemical measurements

Coin-type cells (CR2032) were assembled for symmetric Zn||Zn cells, Zn||Ti and Zn||Cu half cells with the glass fiber as the separator. Full cells were assembled using Zn plate as anode, PANI as cathode, glass fiber as separator in coin-type cells (CR2032) and pouch cells (6 cm × 8 cm). Linear polarization was measured by scanning between -0.2 and 0.2 V (vs. the open circuit potential) at 1 mV s^{-1} using symmetric Zn||Zn cells. Cyclic voltammetry (CV) tests were

conducted on an Admiral instruments electrochemical workstation in the voltage range of -0.2~0.3 V (vs. Zn/Zn^{2+}) for Zn‖Cu half cells in different electrolytes. The electrochemical impedance spectroscopy (EIS) was measured with a frequency range from 100 kHz to 0.05 Hz and an AC amplitude of 10 mV using an Admiral instruments electrochemical workstation for symmetric Zn‖Zn cells. The Coulombic efficiencies (CE) of the Zn‖Ti cells were measured at 10 mA cm^{-2} with a fixed cycling capacity of 10 mA h cm^{-2}. Linear sweep voltammetry was conducted in a three-electrode configuration at 10 mV s^{-1}, with Pt foil as the working electrode and counter electrode, and Ag/AgCl as the reference electrode.

1.4 Theoretical Calculations

Quantum chemistry calculations: Density functional theory (DFT) simulation was performed via Gaussian 16 software package. The structures of molecules were optimized at the B3LYP/SDD level for Zn and B3LYP/6-31G + (d, p) level for other elements. Frequency calculations at the same level of theory were performed to determine the nature of a stationary point as the true local minimum.

The binding energy (BE) between Zn^{2+} and DPA (or H_2O) molecular is defined as following:

$$BE = E_{Zn\text{-}DPA\ (or\ H2O)} - E_{Zn} - E_{DPA\ (or\ H2O)}.$$

Where $E_{Zn\text{-}DPA\ (or\ H2O)}$, $E_{DPA\ (or\ H2O)}$, and E_{Zn} correspond to the total energy of the complex of Zn-DPA (or H_2O), DPA (or H_2O), and Zn, respectively. All calculated results of molecular electrostatic potential (MESP) were performed with Multiwfn 3.9 programs. All visualization of MESP plots was carried out by Visual Molecule Dynamics (VMD) software.

Ab-initial calculations: The calculations related to the interaction between Zn crystal and molecules were carried out using the Vienna ab initio simulation package (VASP) within the projector augmented wave (PAW) potentials for core electrons and the Perdew-Burke-Ernzerhof (PBE) form of the generalized gradient approximation (GGA) for exchange and correlation functional. An energy cutoff of 450 eV was used for the plane wave expansion of valence electron wave functions. The Brillouin zone was sampled using a Monkhorst-Pack special k-point mesh of Γ-centered $2 \times 2 \times 1$ for all the structure optimizations. If not specified, a vacuum layer of 30 Å was introduced to avoid interactions between the simulated Zn supercell of $5 \times 5 \times 1$ and the periodic images. All structures were relaxed, with all atoms allowed to move until the force on each atom was less than 0.035 eV/Å.

The absorbed energy between Zn slab and DPA (or H_2O) was defined as following equation:

$$E_{ads} = E_{Zn\text{-}DPA\ (or\ H2O)} - (E_{Zn} + E_{DPA\ (or\ H2O)})$$

Where $E_{Zn-DPA/H2O}$ stands for the total energy of DPA (or H_2O) adsorbed on the Zn layer, E_{Zn} is the energy of Zn layer, $E_{DPA\ (or\ H2O)}$ is the energy of DPA (or H_2O).

2. Supplementary Results
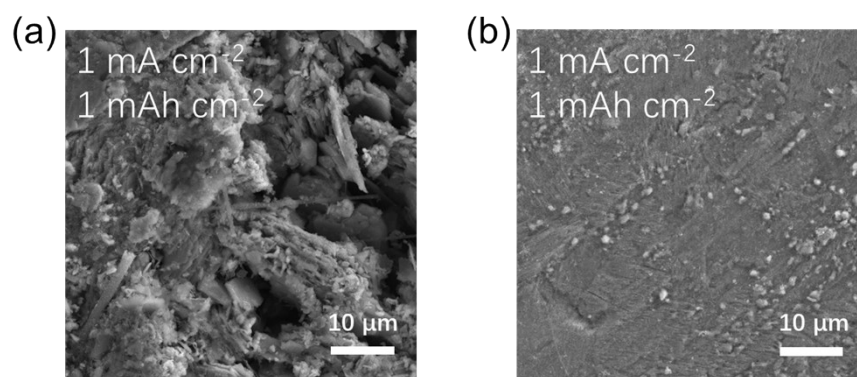

Figure S1. SEM images of Zn anode cycled in (a) ZSO and (b) ZSPA electrolyte for 50 cycles under 1 mA cm^{-2} and 1 mAh cm^{-2}.
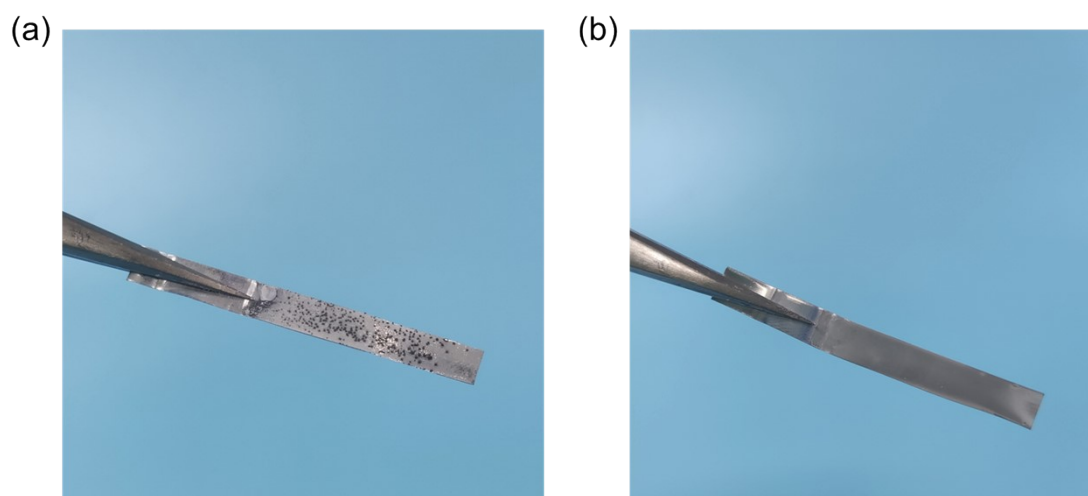
Figure S2. Photographs of Zn anode after plating in (a) ZSO and (b) ZSPA electrolyte under 15 mA cm^{-2} for 30 min. Obviously, various random protrusions were dramatically formed in ZSO electrolyte. In sharp contrast, while the Zn deposits plated in ZSPA electrolyte demonstrated a dense, smooth surface morphology.
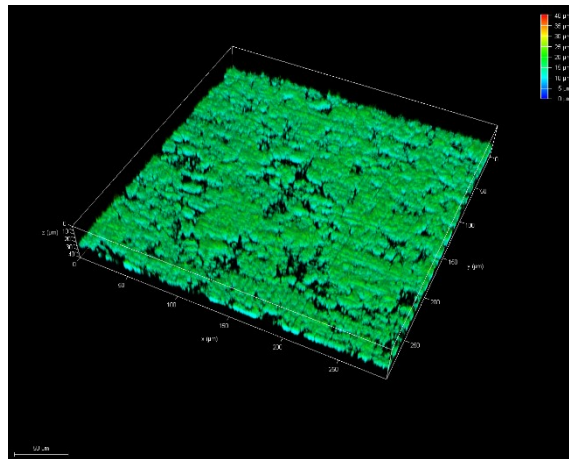
Figure S3. LCSM image of the pristine Zn plate shows the altitude intercept on the surface is ~12 μm.
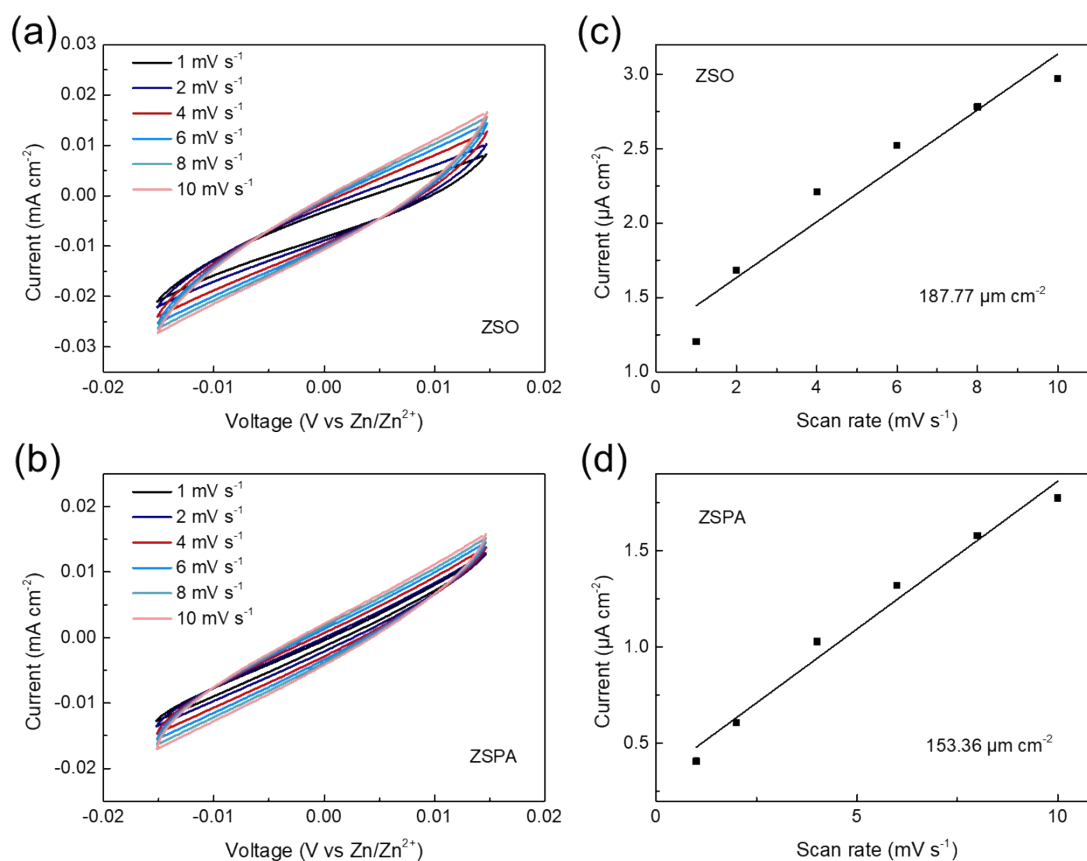
Figure S4. Double layer capacity measurements for Zn substrates in ZSO and ZSPA electrolytes. (a-b) Cyclic voltammograms curves for symmetric Zn‖Zn cells in (a) ZSO and (b) ZSPA electrolyte in a voltage range of -0.015 V to 0.015 V under various scanning rates. (c-d) Plots of capacitive currents versus scan rates and the corresponding electric double-layer capacitance in (c) ZSO and (d) ZSPA electrolyte. The double layer capacitance was calculated through $C = i_c/v$. In CV scans, double layer current $i_c=dq/dt=d(C\varphi)/dt=C(d\varphi/dt)+\varphi(dC/dt)$, $dC/dt=0$, $d\varphi/dt=$scan rate (v). So $i_c=Cv$. The linear dependence of the capacitive current (i_c) on scan rate (v) can be used to determine the capacity. Capacity (C) is obtained from the slope of the i_c versus v graphs. Here, we choose $i_c = (i_{0v+} - i_{0v-})/2$. It is half value of current difference during forward scan and negative scan at 0 V.[2]
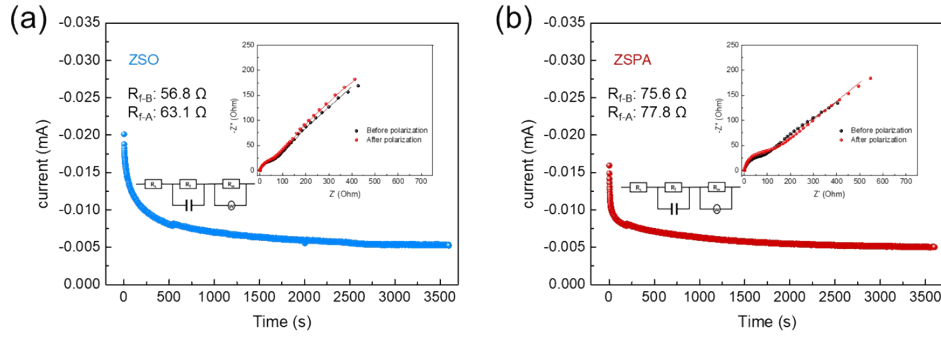
Figure S5. Current-time plots of symmetrical Zn‖Zn cells in (a) ZSO and (b) ZSPA electrolyte after polarization at a constant potential (10 mV) for 3600s. Insets are the impedance spectra before and after the polarization. The transference number of Zn^{2+} (t_{Zn-ion}) was determined by the following equation:

$$t_{Zn-ion} = \frac{I_s(\Delta V - I_0 R_0)}{I_0(\Delta V - I_e R_e)}$$

Where ΔV is the applied voltage (10 mV); I_0 and R_0 are the initial current and resistance, respectively; I_e and R_e are the steady-state current and resistance, respectively.[3] The calculated t_{Zn-ion} for ZSO-based cell and ZSPA-based cell are 0.28 and 0.34, respectively.
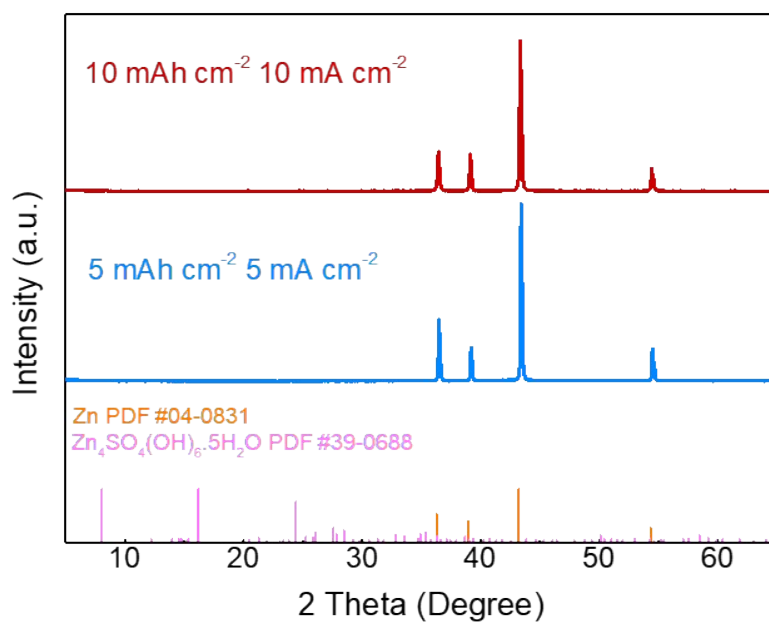
Figure S6. XRD patterns of Zn anodes after 50 plating/stripping cycles in ZSPA electrolyte under different cycling conditions.
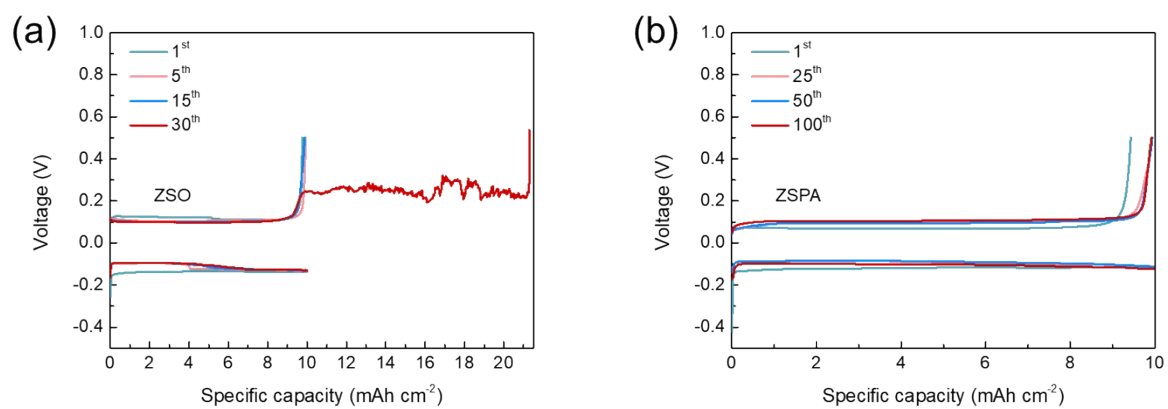
Figure S7. Voltage profiles of the Zn||Ti cells at various cycles in (a) ZSO and (b) ZSPA electrolyte at 10 mA cm^{-2} and 10 mAh cm^{-2}.
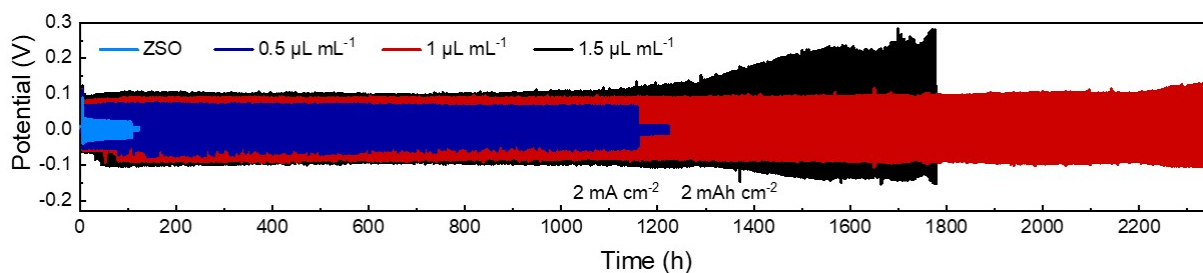
Figure S8. Cycling performance of symmetric Zn||Zn cells in ZSO electrolyte with different contents of DPA additives at 2 mA cm^{-2}, 2 mAh cm^{-2}. Obviously, the best cyclying performance was obtained in ZSO electrolyte with 1 μL mL^{-1} DPA additive. The less DPA additive (0.5 μL mL^{-1}) can lower the polarization potential, but the cycle life was shortened (~1158 h at 2 mA cm^{-2} and 2 mAh cm^{-2}), possibly because such a low content of DPA additive could not modulate the whole surface of Zn anode. On the contrary, too many DPA additives (1.5 μL mL^{-1}) would further increase the polarization potential, which goes against the cyclic stability of the Zn anode. Therefore, the concentration of 1 μL mL^{-1} was selected as optimal concentration.
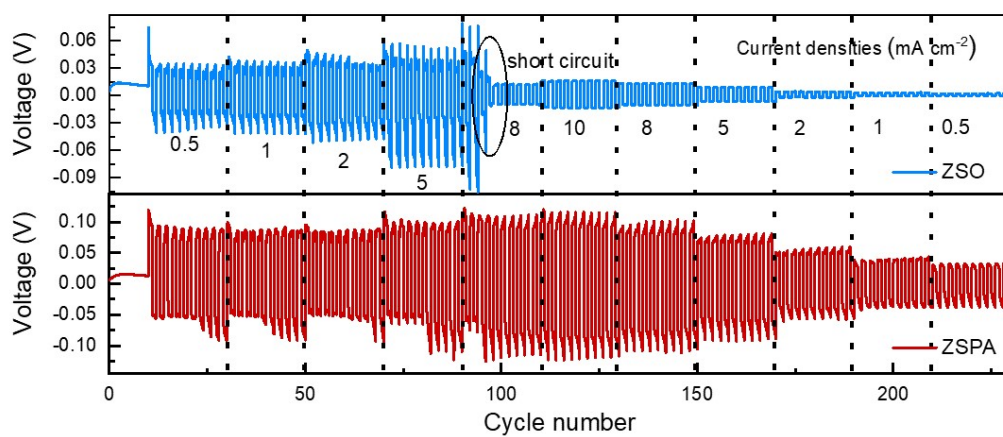
**Figure S9.** The rate performance of symmetric Zn||Zn cells using ZSO and ZSPA electrolyte.

(a)

10 μm

50 μm

(b)

10 μm

50 μm
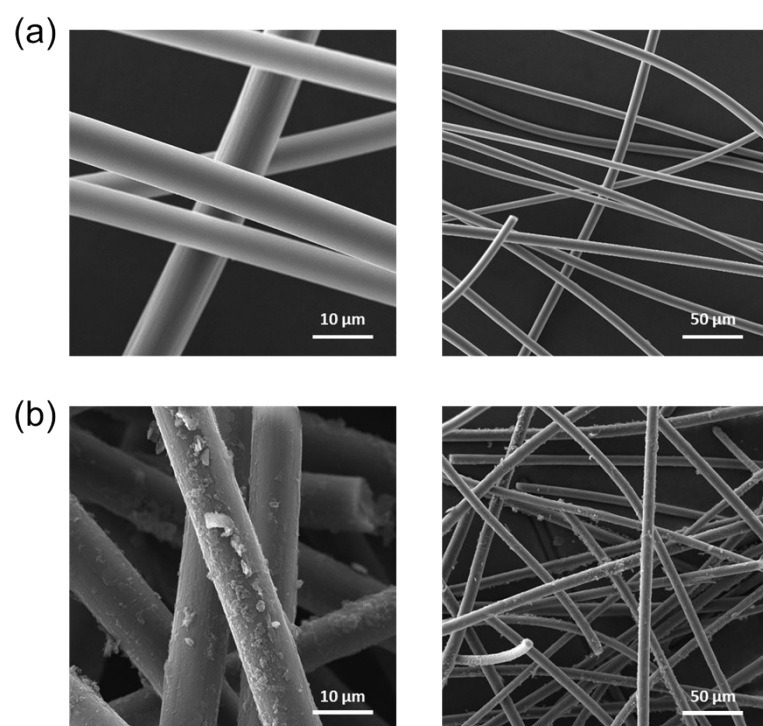
**Figure S10.** SEM images of (a) the pristine carbon felts and (b) PANI coated carbon felts.
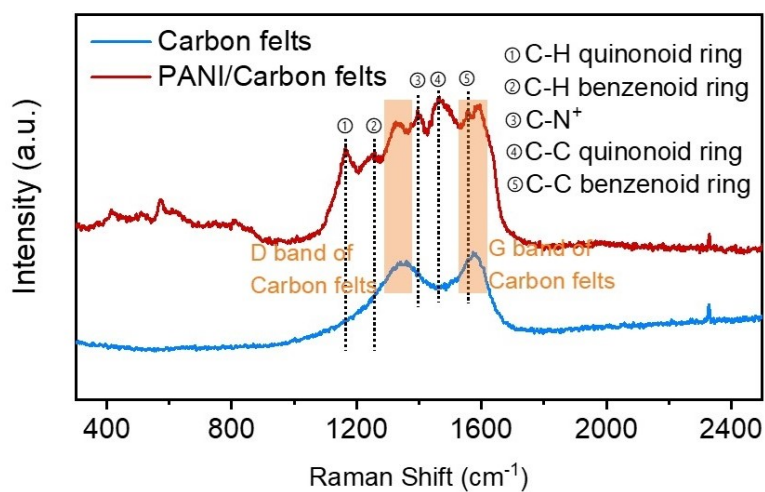
Figure S11. Raman spectra of carbon felts and the as-prepared PANI cathode. In the Raman spectrum of PANI, the characteristic peaks of PANI are observed at 1162 (C-H bending vibrations of quinoid ring), 1212 (C-H bending vibrations of benzenoid ring), 1480 (C-C stretching vibrations of quinoid ring), 1590 (C-C stretching vibrations of benzenoid ring), and 1330 cm^{-1} (stretching vibration of C-N$^+$), respectively, suggesting the existence of PANI on the carbon felts.
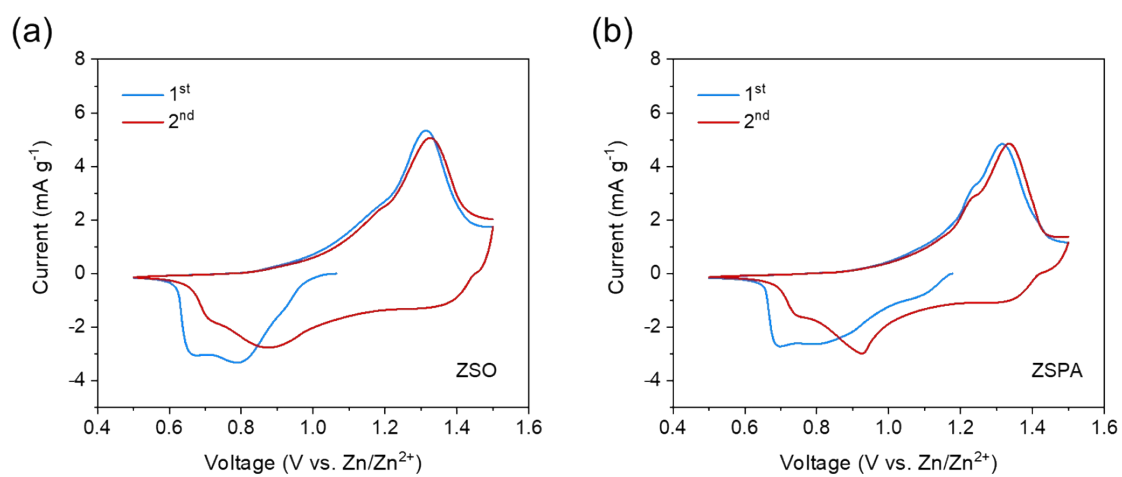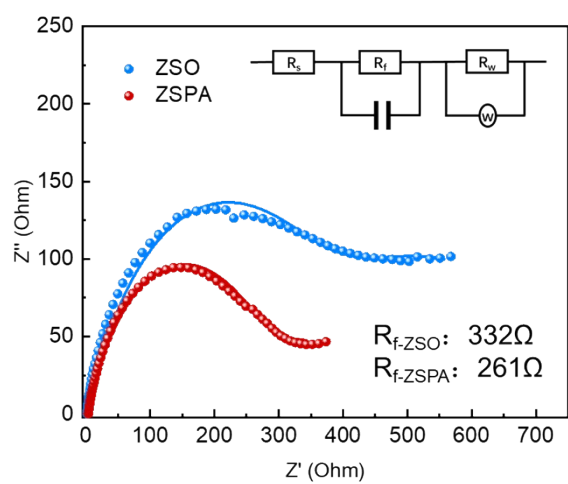
Figure S12. The CV curves of the Zn∥PANI full cells in (a) ZSO and (b) ZSPA electrolyte under 2 mV/s.
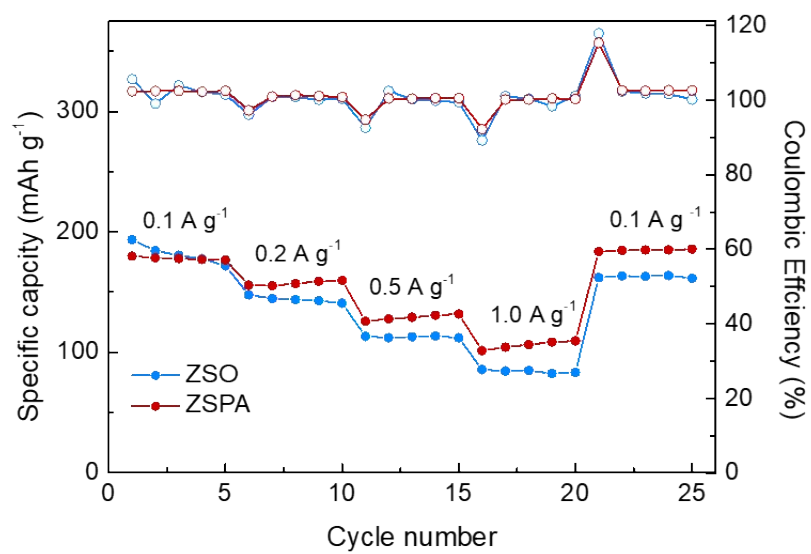
Figure S13. Rate performance for Zn||PANI coin cells in different electrolytes.

Figure S14. EIS spectra of the Zn‖PANI full cells in ZSO electrolyte with/without DPA additive.

References

1   F. Wan, L. Zhang, X. Wang, S. Bi, Z. Niu, J. Chen, *Adv. Funct. Mater.*, 2018, **28**, 1804975.

2   Y. Jin, K. S. Han, Y. Shao, M. L. Sushko, J. Xiao, H. L. Pan, J. Liu, *Adv. Funct. Mater.*, 2020, **30**, 2003932.

3   J. Hao, B. Li, X. Li, X. Zeng, S. Zhang, F. Yang, S. Liu, D. Li, C. Wu, Z. Guo, *Adv. Mater.*, 2020, **32**, 2003021.